# A New Method for Direction Finding of Elliptically Polarized VLF Waves

*By*

Koichiro TSURUDA and Kanji HAYASHI*

*Summary*: A new method has been developed for the direction finding of elliptically polarized VLF electronmagnetic waves. The method uses simple algebraic relations between the vertical electric fields and the horizontal magnetic field of the incident wave to eliminate the TE component of the magnetic field. The present method can give a reasonably accurate estimate of the angle of incidence as well as azimuth when the incident wave is elliptically polarized, and this is complementary to the classical goniometer technique which is suited for the direction finding of the linearly polarized waves. Preliminary experimental result on the direction finding of whistlers by this newly developed technique is also reported.

## 1. INTRODUCTION

From the early stage of investigation on the natural VLF wave phenomena the question of the arrival direction of the wave has attracted much interest. The most simple and widely used technique of the VLF direction finding is to use the crossed loop goniometer and find the angle where the signal strength attains minimum. Watts (1959) was the first to show that some whistlers exhibit null when the goniometer is rotated, and Ellis and Cartwright (1959) used this technique to derive the arrival direction of VLF emissions.

The crossed loop goniometer, which is equivalent to one rotating loop, can give a correct azimuth angle when the incident wave is linearly polarized. However, as the wave polarization departs from linearity the error in the estimated azimuth increases. Moreover, the information on the zenith angle of the incident wave vector cannot be derived from the output of goniometers. Bullough and Sagredo (1973) have overcome the latter shortcomming of the goniometer method by obtaining the L value of the whistler path by the nose frequency technique, and succeeded in determining the location of the exit point (i.e. the point where the wave leaves the ionosphere) of nose whistlers. Their method is effective if the exit point is located far away from the observation site, but it is not free from the inherent shortcomming of the goniometer method when the exit point is close to the observation site and the wave polarization becomes an ellipse. In addition, the nose frequency method can not be employed in low latitudes.

---

* Geophysics Research Laboratory, University of Tokyo.

More sophisticated direction finding studies of whistlers have been carried out by Delloue and his co-workers (Delloue et al., 1963) who used a spaced receiver technique. This method, however, seems to be difficult to practice as it requires a very high accuracy in the time measurements and the signal to noise ratio higher than what is normally achieved in natural VLF wave observations.

Another more basic approach to the direction finding of obliquely incident VLF waves has been made by Tanaka (1972) who eliminated the TE (transverse electric component in the output signal of loop antennas by reading the loop output at the moment when the vertical component of the electric field $E_z$ (which consists of TE mode) crosses the zero line. He applied this technique to derive the direction of VLF emissions, but this method requires the observed wave to be monochromatic. Contamination of the signal by random noises and waves with different frequencies will seriously degrade the accuracy of the results.

In the present paper we shall present a new method of the direction finding in which the TE-mode is eliminated by taking a simple algebraic combination of the observed wave fields. This method gives a reasonable accurate direction for non-monochrmatic waves and is not influenced by the conductivity of the ground. The preliminary experimental result by this method is also reported.

## 2. PRINCIPLE OF THE DIRECTION MEASUREMENT AND BRIEF DISCRIPTIONS OF THE EQUIPMENTS

We define the bracket operator $[A, B]$ as

$$[A, B] = \frac{i}{2}(A \cdot B^* - A^* \cdot B) \tag{1}$$

where the asterisk denotes the complex conjugate. In the free space $E_z$ of the plane monochromatic wave is related to the horizontal components $H_x$ and $H_y$ of the magnetic field as

$$E_z = -n_x H_y + n_y H_x \tag{2}$$

where $n_x$ and $n_y$ are the horizontal components of the wave normal vector which can be written as

$$\begin{aligned} n_x &= \sin \theta \cos \phi \\ n_y &= \sin \theta \sin \phi \end{aligned} \tag{3}$$

in the coordinate system of Fig. 1.
Using equation (2) we have

$$\begin{aligned} [E_z, H_x] &= \frac{i}{2} n_x (H_x H_y^* - H_x^* H_y) \\ &= n_x [H_x, H_y] \end{aligned} \tag{4}$$
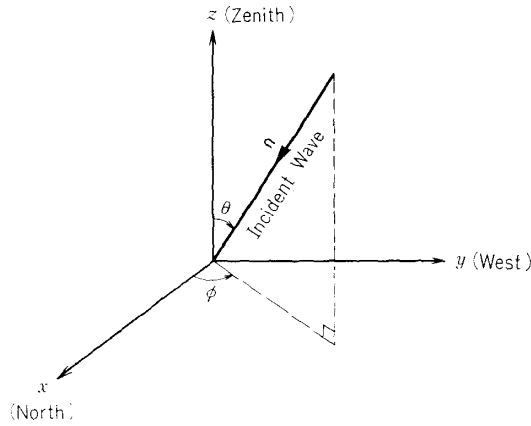
$$[E_z, H_y] = n_y [H_x, H_y]$$

FIG. 1.  Coordinate system.

When the wave polarization is linear $[E_z, H_x]$, $[E_z, H_y]$ and $[H_x, H_y]$ vanish and equation (4) loses its meaning.  However, so far as the wave is elliptically polarized both sides of equation (4) remain finite and we can easily find the horizontal components $n_x$ and $n_y$ of the wave normal by dividing $[E_z, H_x]$ and $[E_z, H_z]$ by $[H_x, H_y]$.  The value of $n_z$ follows from the relation $n_x^2 + n_y^2 + n_z^2 = 1$.

In the actual situation of the direction finding, however, some complexities have to be taken into account.  The wave fields observed are composed of incident and reflected waves and the reflection coefficient of the ground is large for VLF waves.  Whistlers and VLF emissions are by no means monochromatic and consist of waves with different frequencies and different phases.  Let us first consider the case where there are multiple waves coming from the same direction.  The ground reflection is assumed to occur only at the observing site, and the earth is considered to be flat.  Then the incident and reflected waves have the same $n_x$ and $n_y$, and the mixture of waves can be written as;

$$(E_z, H_x, H_y) = \sum_i (e_{zi}, h_{xi}, h_{yi})$$

where

$$e_{zi} = -n_x h_{yi} + n_y h_{xi} \tag{5}$$

Substituting (5) into (1), we obtain for observed wave $(E_z, H_x, H_y)$ the same expression as (4);

$$
\begin{aligned}
[E_z, H_x] &= \frac{i}{2}\Bigg\{\Bigg(-n_x \sum_i h_{yi} + n_y \sum_i h_{xi}\Bigg) \cdot \sum_j h_{xj}^* \\
&\quad -\Bigg(-n_x \sum_i h_{yi}^* + n_y \sum_i h_{xi}^*\Bigg) \cdot \sum_j h_{xj}\Bigg\} \\
&= n_x \cdot \frac{i}{2}\Bigg(\sum_i h_{xi} \cdot \sum_j h_{yj}^* - \sum_i h_{xi}^* \cdot \sum_j h_{yj}\Bigg) \\
&= n_x[H_x, H_y] \\
[E_z, H_y] &= n_y[H_x, H_y]
\end{aligned}
\tag{6}
$$

Thus we can find the wave normal vector $n$ from observed fields $(E_z, H_x, H_y)$ regardless of the ground reflection at the observing site and the non-monochromacity of the incident waves.

The reflection of the wave occurs, however, also at the ionosphere. Coupled with the ground reflection this gives rise to multiple reflections of the original signal and introduces error in the estimate of the normal vector of the wave coming directly from the exit point. It is shown in Appendix A, however, that the extent of this error is reasonably small.

Equation (1) is equiavlent to the following relation between real parts of $A$ and $B$

$$[A, B] = A_r \tilde{B}_r - \tilde{A}_r B_r \qquad (7)$$

where $\tilde{A}_r$ and $\tilde{B}_r$ are produced by advancing the phase of $A_r$ and $B_r$ by 90 degrees. In the monochromatic case, $A_r$ and $B_r$ can be written as;

$$\begin{aligned} A_r &= A_{r0} \cos \omega t \\ B_r &= B_{r0} \cos (\omega t + \alpha) \end{aligned} \qquad (8)$$

By substituting (8) into (7) we obtain

$$[A, B] = A_{r0} B_{r0} \sin \alpha \qquad (9)$$

This is equal to the two times of DC part of $A_r \tilde{B}_r$ and (7) can be written as

$$[A, B] = 2(A_r \tilde{B}_r) \qquad (10)$$

When the wave is not monochromatic and composed of waves with amplitudes $a_i$ and $b_i$, frequency $\omega_i$ and phases $\alpha_i$ and $\beta_i$, namely,

$$\begin{aligned} A_r &= \sum_i a_i \cos (\omega_i t + \alpha_i) \\ B_r &= \sum_i b_i \cos (\omega_i t + \beta_i) \end{aligned} \qquad (11)$$

we have;

$$[A, B] = \sum_{i,j} a_i b_j \sin \{(\omega_i - \omega_j)t + (\alpha_i - \beta_j)\} \qquad (12)$$

$$A_r \tilde{B}_r = \tfrac{1}{2} \sum_{i,j} a_i b_i [\sin \{(\omega_i - \omega_j)t + (\alpha_i - \beta_j)\} \\ + \sin \{(\omega_i + \omega_j)t + (\alpha_i + \beta_j)\}] \qquad (13)$$

The maximum frequency of (12) is equal to the band width $\Delta \omega$ of $A_r$ and $B_r$. If $\omega_i + \omega_j$ is sufficiently higher than $\Delta \omega$ the second term in the bracket of equation (13) can be suppressed by a low pass filter and equation (10) can be made to hold. Hence equation (4) can be replaced by;

$$\begin{aligned} n_x &= \frac{(E_z \tilde{H}_x)}{(H_x \tilde{H}_y)} \\ n_y &= \frac{(E_z \tilde{H}_y)}{(H_x \tilde{H}_y)} \end{aligned} \qquad (14)$$
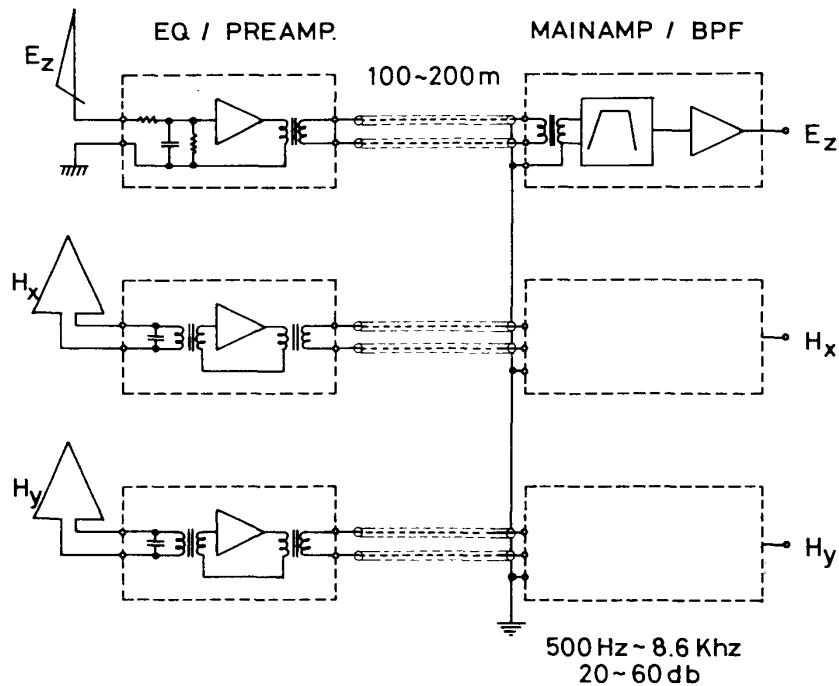
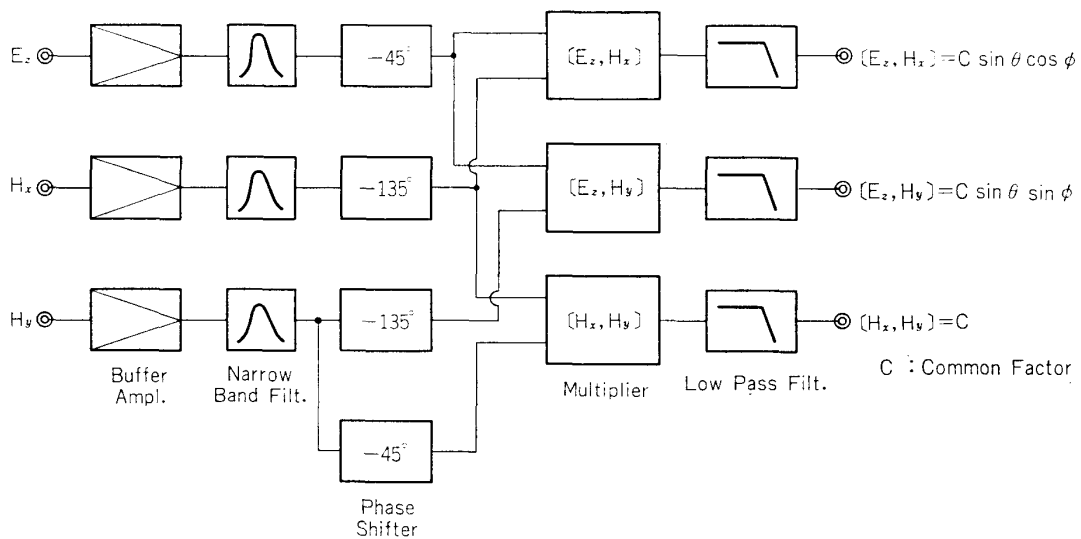FIG. 2.   Schematic illustration of VLF receiver.

FIG. 3.   Schematic illustration of VLF direction analyzer.

By using (14) instead of (7) we can reduce the number of phase shifting networks and multiplier circuits.

The receiving equipments of VLF waves used are essentially the same as those employed for usual VLF observations and consist of two loop antennas plus one vertical antenna that receives $E_z$ component. The schematic summary of the present receiving system is given in Fig. 2.
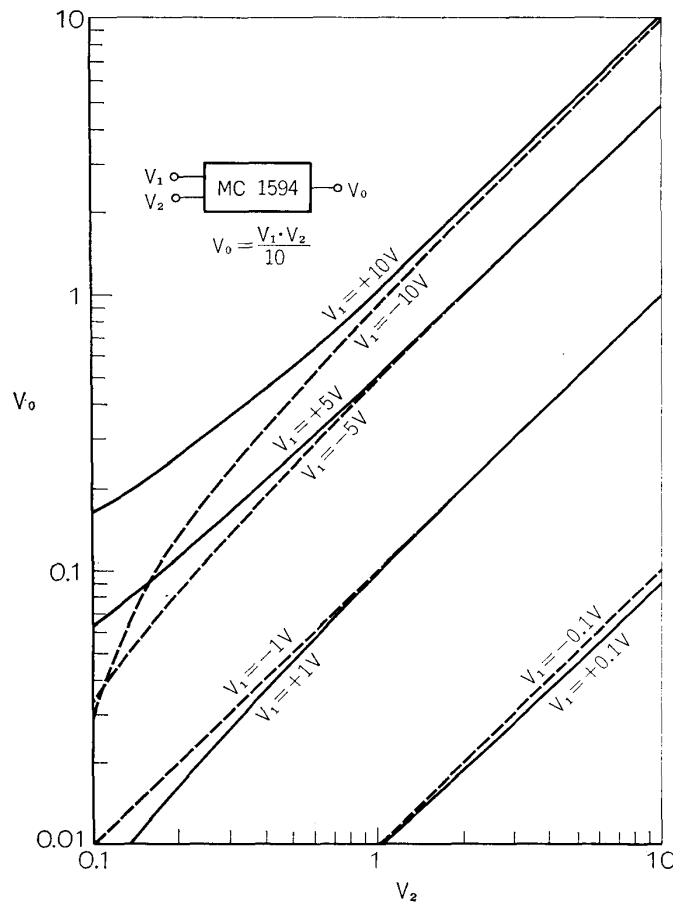
FIG. 4. Input-output characteristics of integrated analog multiplier model MC 1594.

Since equation (14) is sensitive to both relative phase and relative amplitude of three components of the wave field, special care must be paid to equalize the response of the three antennas. We inserted the equalizing network between the antenna terminal and the preamplifier and equalized the response at the expense of sensitivity. The detail of the equalizing network is discussed in the Appendix B.

The block diagram of the direction analyzer is shown in Fig. 3. The band width of the narrow band filter is chosen to be 600 Hz. However, this might have to be changed according to the nature of the source. The center frequency of the filter can be changed by heterodyne method from 0.5 kHz to 10 kHz. The phase shifter network is the usual CR type and $A_r$ is lagged by $-135°$ and $\tilde{A}_r$ by $-45°$ to widen the region where the phase difference between $A_r$ and $\tilde{A}_r$ is $90°$. The model MC 1594 analog multiplier of Motrola Inc. was employed whose input-output characteristics are shown in Fig. 4. As is seen from the figure the input swing in which the accuracy is guranteed is about 30 db. As the straightforward division of $(E_z \tilde{H}_x)$ by $(H_x \tilde{H}_y)$ tend to emphasize the part where $(H_x \tilde{H}_y)$ is small and enhance the error that may exist there, instead, we are going to use the following relations to derive $n_x$ and $n_y$.

$$\frac{\int (E_z \tilde{H}_x) \cdot (H_x \tilde{H}_y) dt}{\int (H_x \tilde{H}_y)^2 dt}$$

$$\frac{\int (E_z \tilde{H}_y) \cdot (H_x \tilde{H}_y) dt}{\int (H_x \tilde{H}_y)^2 dt}$$

## 3. PRELIMINARY RESULTS OF THE DIRECTION FINDING OF WHISTLERS

A preliminary experiment on the direction finding of whistlers were carried out at Kakioka (26°N in geomagnetic latitude) on 20 Feb. 1974. The whistler activity
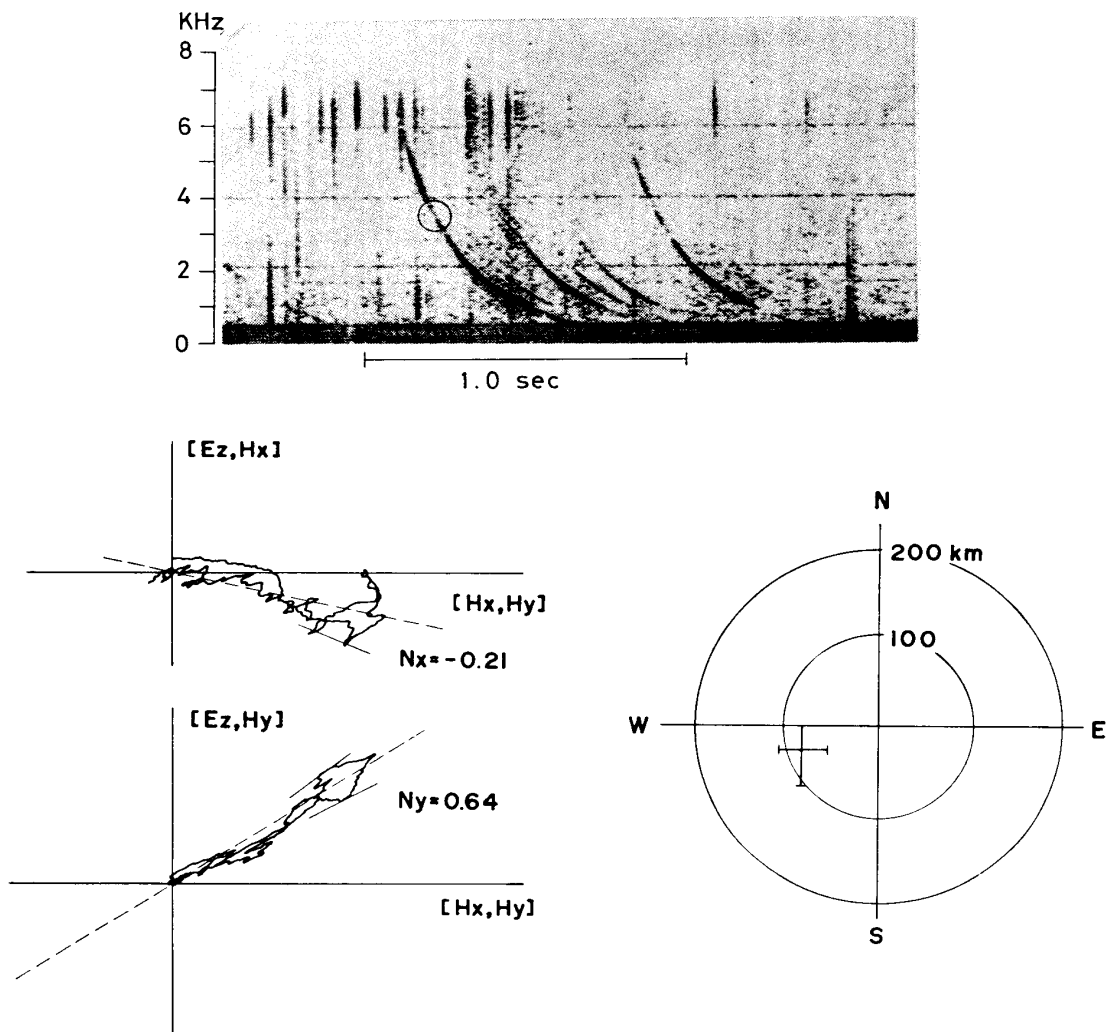
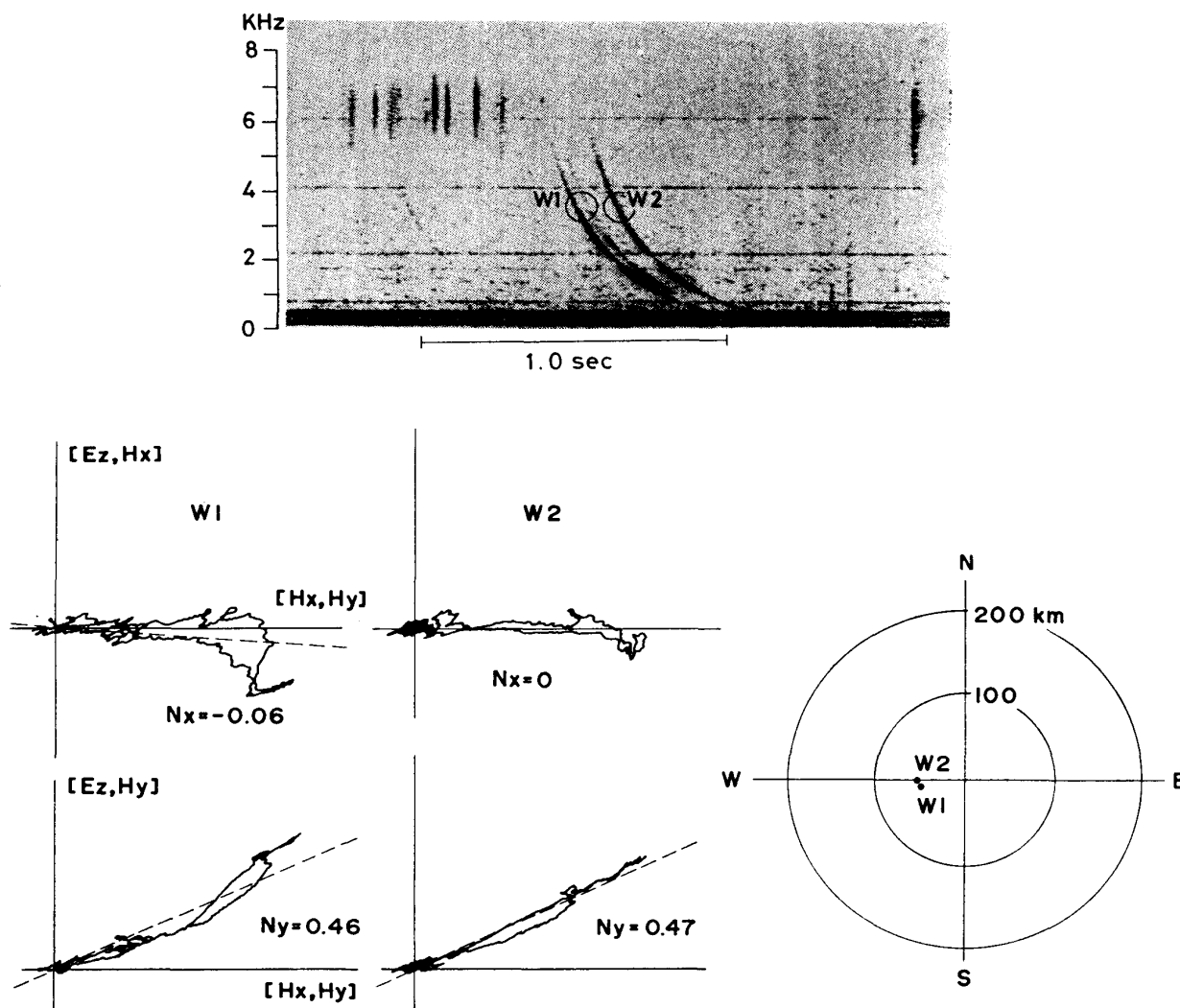NO I     KAKIOKA '74 Feb. 20 14:35 at 3.5 kHz

FIG. 5. Top; Sonagram of whistlers. The analyzed portion is enclosed by a circle.
Bottom left; The variation of $(E_z \tilde{H}_x)$ and $(E_z \tilde{H}_y)$ versus $(H_x \tilde{H}_y)$, the mean slope of which represents $n_x$ and $n_y$, respectively.
Bottom right; Exit point of whistler. The height of the ionosphere is assumed as 100 kilometers.
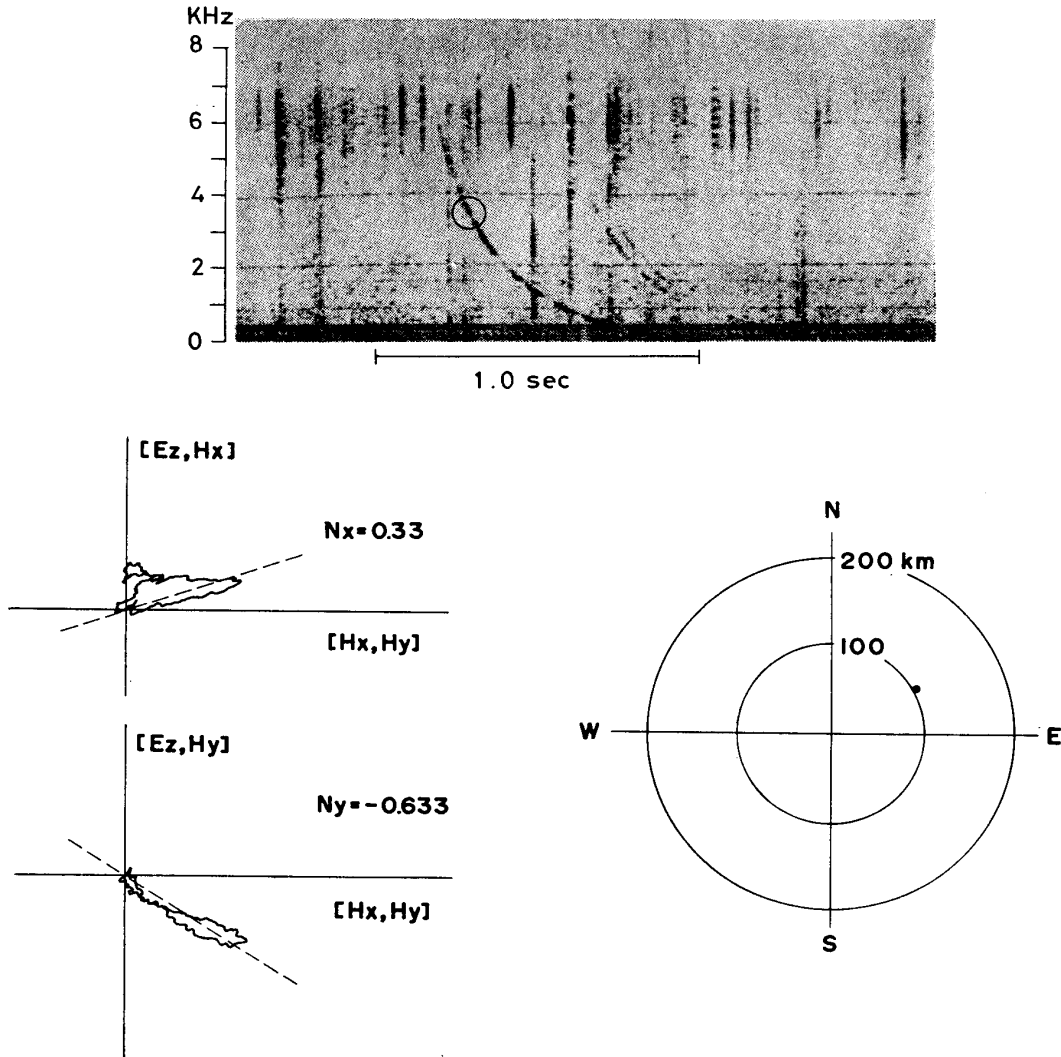
Fig. 6. Same as Fig. 5.

was considerably high throughout that day and most of whistlers recieved were pure-tone whistlers. The reciever output in the frequency band of 3.5 kHz±300 Hz was fed to the direction analyzer. The whistler intensity within that frequency band is roughly 20 db above the noise level for the $E_z$ reciever, though it is only 10–15 db above for the two magneitc fields recievers. To inspect the qaulity of the data as well as the direction of the wave normal, we employed the $X-Y$ presentation of $(E_z\tilde{H}_x)$ and $(H_x\tilde{H}_y)$ as well as $(E_z\tilde{H}_y)$ and $(H_x\tilde{H}_y)$. In the ideal case where the incident whistler wave comes from one direction and there are no noises superposed on them, the $X-Y$ presentation of those parameters should describe a straight line. The slope of $(E_z\tilde{H}_x)-(H_x\tilde{H}_y)$ trajectory is $n_x$ and that of $(E_z\tilde{H}_y)-(H_x\tilde{H}_y)$ is $n_y$. Actually, those trajectories are not straight lines but they draw zigzag curves as seen in the bottom left pannel of Fig. 5, 6, 7 and 8. However, the departure of the curves from the straight line is reasonably small for the cases shown in the Fig. 5, 6 and 7.
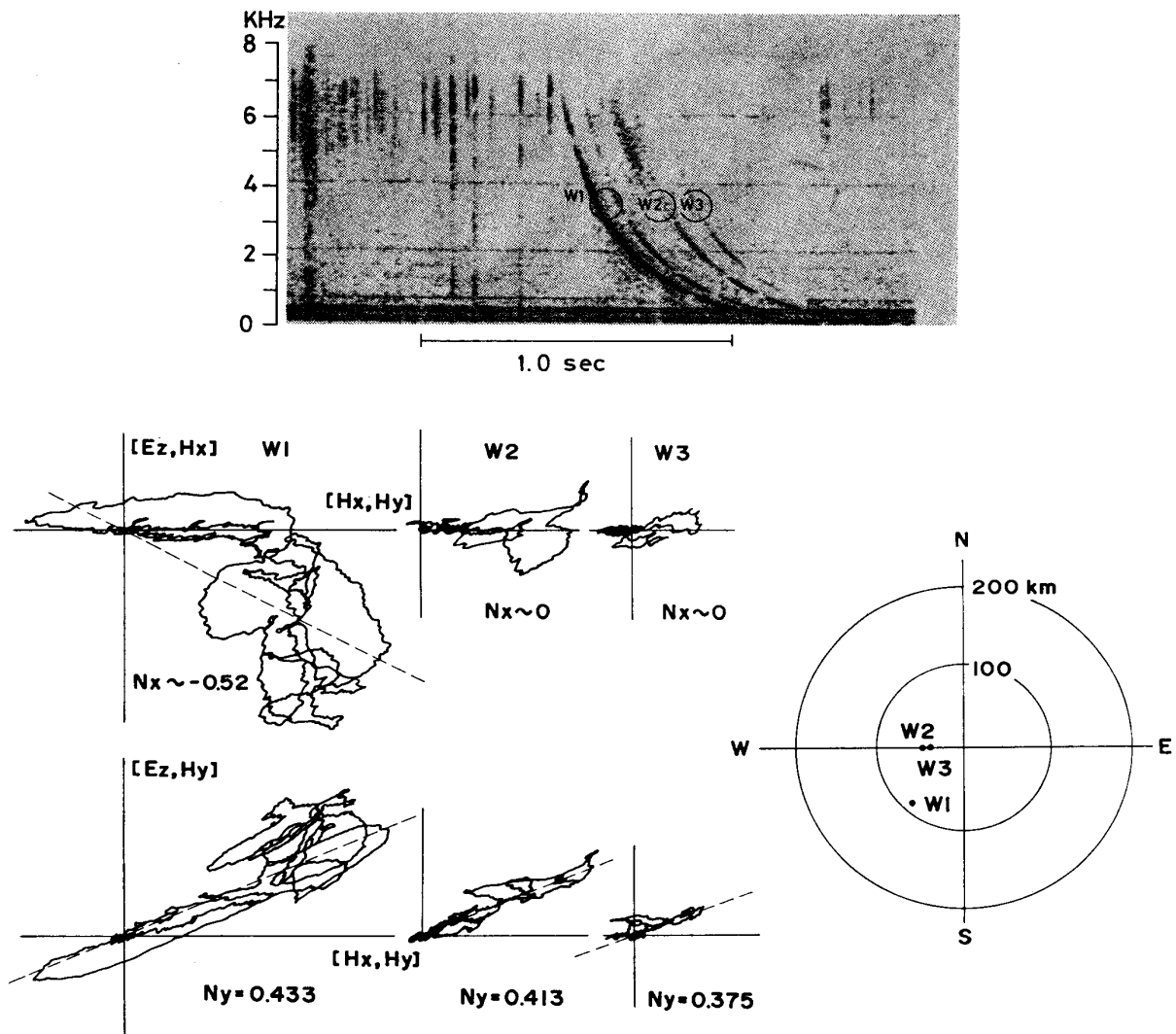
NO 3     KAKIOKA   '74  Feb. 20  14:38  at 3.5 kHz

FIG. 7.  Same as Fig. 5.

We can determine $n_x$ and $n_y$ from the mean slope of these curves.

In the Fig. 5, the analyzed portion of the whistler trace is enclosed by a circle in the sonagram shown in the top pannel. The $n_x$ and $n_y$ determined from the mean slope are −0.21 and 0.64, respectively. By assuming the height of the ionosphere as 100 km we determined the exit point of this wihstler. The exit point is shown in the bottom right pannel where the error bars are estimated from the extent of scatter of the $X−Y$ plots. Fig. 6 is simillar to Fig. 5. The intensity is weaker and the direction is opposite to that of the previous example. Next example shown in Fig. 7 includes three whistler traces. The first two whistlers (noted as W1) are too closely spaced and cannot be separately analyzed by the present choice of the analyzer parameters. W1 and W2 show almost the same direction, the width of $X−Y$ traces

NO 4        KAKIOKA '74 Feb. 20 14:39 at 3.5 kHz

FIG. 8.  Same as Fig. 5.

of W1 being somewhat larger than that of W2. An example of intense whistlers is shown in Fig. 8. The sonagram shows many whistler traces. W1 includes three whistlers and one click due to the atmospherics. W2 includes two traces and W3 includes one faint trace. The $(E_z \tilde{H}_x) - (H_x \tilde{H}_y)$ trajectory of W1 spreads over a wide region. The reason of this wide spreading has not yet been understood. The wide areal extent of the exit regions of those whistlers can be considered as the probable cause of the spread.

From the examples shown in these figures, we may conclude that; 1) for most of whistlers the exit point can be determined by the present direction finding technique with a reasonable accuracy, 2) some of whistlers appears to come from above even at the low latitude stations as Kakioka, and 3) the exit point of some whistlers may have a large area.

## 4. DISCUSSIONS

Though we have calibrated the recieving system by means of dummy antennas, some ambiguities remain in the estimated capacitance and effective height of vertical antenna. Therefore, an absolute calibration of the system will be the subject for a future study. Unfortunately, there are no VLF radio sources that can be used for the absolute calibration of the system, so that the calibration must be carried out by indirect methods. The discrepancy in phase shift between electric field reciever and magnetic field reciever caused by mal-estimate of the antenna capacitance is relatively small. For example, in the present case of antenna parameters the additional phase shift in $E_z$ reciever at 3.5 kHz is only 3.6 degrees when the antenna capacitance is changed by 20 per cent. The accuracy of azimuth angle does not depend upon the discrepancy of the sensitivity between $E_z$ reciever and magnetic field reciever. Hence, the measured azimuth angle can be considered as accurate regardless of the absolute calibrations. On the other hand, the accuracy of $\theta$ directly depends upon the accuracy in equalization of sensitivities of two recievers. Comparatively simple method of the accuracy test for $\theta$ measurement is that which uses three direction finders settled some hundreds of kilometers apart from each other. Observing the azimuth of the same whistler event by the three direction finders we shall be able to determine the location and extent of the exit area of the whistler with no regard to the angle of incidence. If the exit area thus determined is sufficiently small we may use the whistler as a test signal for $\theta$ mesurements.

The spaced observations of whistlers by two or three calibrated direction finders will, in turn give the information about the extent of the source regions in the ionosphere. This will contribute to the study of whistler duct or small scale irregularities in the ionosphere.

The tracking of the exit points of whistlers by the direction finder will provides an interesting information about the drift motions of thermal plasma in the magnetosphere. The exit point of a whistler moves in accordance with the motion of the duct through which the whistler has propagated. The ducts move with the surrounding thermal plasma according to the electric field there. Hence we shall be able to obtain the data of vector electric field in the magnetosphere. This will be an extention of Carpenter's nose whistler method in deducing the cross L drift of whistler duct (Carpenter and Stone, 1967).

It is generally believed that the occurrence of auroral hiss is well correlated to the manifestation of aurora. The comparison of the all-sky camera record to the similar mapping of the exit point of VLF emissions will provides data for the study of generation mechanism of VLF emissions.

According to Yoshino (personal communication), the occurrence frequency of whistlers observed at Sugadaira (26°N) is well controlled by the distribution of clouds near the geomagnetic conjugate point of Sugadaira. Ray tracing of whistlers shows that the paths of non-ducted whistlers are not the same for different frequency components (Maeda and Kimura, 1956). The exit point of a non-ducted whistler, therefore, varies with frequency. This point can be examined by the direction observations of a whistler for several frequencies.

## APPENDIX A

Errors due to multiple reflections

Since both the lower ionosphere and the ground act as a reflector of VLF waves, the waves reflected many times may come to the receiver together with the direct wave. As shown in Fig. A–1 the presence of rays 1, 2, 3, . . . having different wave normals from that of the direct ray 0 can cause error in the direction finding of the ray 0. The wave normal vector $n_i$ associated with the $i$-th ray can be written as;

$$n_{xi} = \sin \theta_i \cos \phi$$
$$n_{yi} = \sin \theta_i \sin \phi \qquad \qquad \text{(A-1)}$$
$$n_{zi} = \cos \theta_i$$

where $\theta_i$ is related to the angle of incidence of the direct ray $\theta_0$ by a simple geometrical relation between the $i$-th ray and the direct ray as;

$$\tan \theta_i = \frac{1}{2i+1} \tan \theta_0 \qquad \qquad \text{(A-2)}$$

The total field $(E_z, H_x, H_y)$ is the summation of the field of all rays and can be written as;

$$(E_z, H_x, H_y) = \sum_i (e_{zi}, h_{xi}, h_{yi}) \qquad \qquad \text{(A-3)}$$

where

$$e_{zi} = -n_{xi}h_{yi} + n_{yi}h_{xi}.$$

Substituting (A–3) into (4) we obtain;

$$[E_z, H_x] = \cos \phi \sum_i \sin \theta_i \sum_j [h_{xi}, h_{yj}] + \sin \phi \sum_i \sin \theta_i \sum_j [h_{xi}, h_{xj}]$$
$$[E_z, H_y] = \sin \phi \sum_i \sin \theta_i \sum_j [h_{xi}, h_{yi}] - \cos \phi \sum_i \sin \theta_i \sum_j [h_{yi}, h_{yj}] \qquad \text{(A-4)}$$
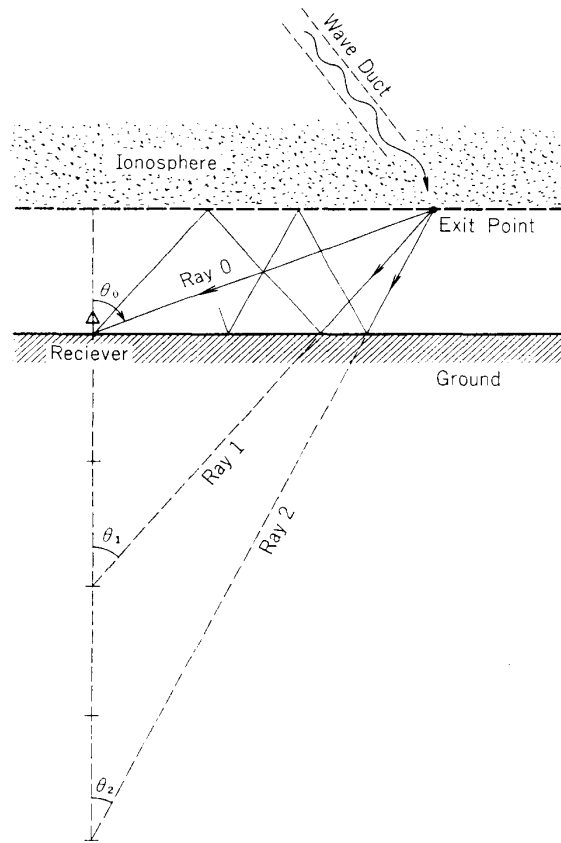$$[H_x, H_y] = \sum_{i,j} [h_{xi}, h_{yj}]$$

FIG. A-1.   Geometry of multiple rays.

The cross terms $[h_{xi}, h_{xj}]$ and $[h_{yi}, h_{yj}]$ remain finite when $i \neq j$ and the second term on the righthand side of (A-4) may become an error source in the estimate of $\phi$. The accuracy of $\theta$ is also limitted by the ratio between $\sin \theta_0 [h_{x0}, h_{y0}]$ and $\sum_{i \neq 1} \sin \theta_i \sum_{j \neq 1} [h_{xi}, h_{yj}]$.

In order to make a rough estimate of these errors we assume that (1) the waves expand spherically after leaving the ionosphere, (2) the reflection coefficients of the ionosphere can be approximated by a scalor reflection coefficient $R$ and the phase change at the reflection can be neglected, (3) the reflection coefficients at the ground is 1. The intensity of $j$-th ray $I_j$, then, can be expressed in terms of the intensity of the direct ray $I_0$ as;

$$I_j = \sqrt{\frac{\tan^2 \theta_0 + 1}{\tan^2 \theta_0 + (2j+1)^2}} \, R^j I_0 \qquad (A-5)$$

The phase of $h_{xj}$ relative to that of $h_{x0}$ is

$$\phi_j = \frac{\omega}{c} H_{eff} (\sqrt{\tan^2 \theta_0 + (2j+1)^2} - \sqrt{\tan^2 \theta_0 + 1}) \qquad (A-6)$$
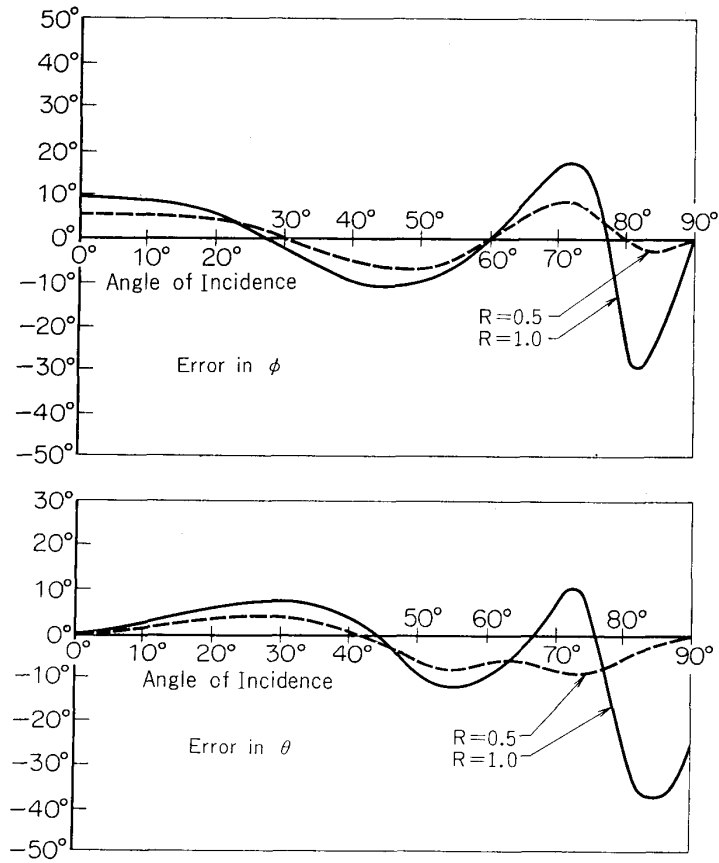
FIG. A-2.  Errors due to multiple reflections.

$$F = 4.0\,\text{kHz} \qquad \phi_0 = \text{Arg}\,(h_{x0}, h_{y0}) = 45^\circ$$

where $H_{eff}$ is the effective reflection height and $c$ is the light velocity.  Denoting the phase angle between $h_{x0}$ and $h_{y0}$ as $\phi_0$, $[h_{xi}, h_{yj}]$, $[h_{xi}, h_{xj}]$ and $[h_{yi}, h_{yj}]$ can be written as;

$$[h_{xi}, h_{yj}] \simeq A_{ij} \sin\,(\phi_i - \phi_j + \phi_0) \cdot |h_{x0}h_{y0}|$$

$$[h_{xi}, h_{xj}] \simeq A_{ij} \sin\,(\phi_i - \phi_j) \cdot |h_{x0}h_{x0}| \qquad\qquad\qquad (\text{A-7})$$

$$[h_{yi}, h_{yj}] \simeq A_{ij} \sin\,(\phi_i - \phi_j) \cdot |h_{y0}h_{y0}|$$

where

$$A_{ij} = \frac{(\tan^2 \theta_0 + 1)R^{i+j}}{\sqrt{\{\tan^2 \theta_0 + (2i+1)^2\}\{\tan^2 \theta_0 + (2j+1)^2\}}}$$

If we express the magnitude of $|h_{x0}h_{y0}|$, $|h_{x0}h_{x0}|$ and $|h_{y0}h_{y0}|$ roughly as $h_0^2$, (A-4) can be written as;

$$[E_z, H_x] = A \cos\,\phi + B \sin\,\phi$$

$$[E_z, H_y] = A \sin\,\phi - B \cos\,\phi \qquad\qquad\qquad (\text{A-8})$$

$$[H_x, H_y] = C$$

where

$$A = \sum_i \sin \theta_i \sum_j A_{ij} \sin (\phi_i - \phi_j + \phi_0) h_0^2$$

$$B = \sum_i \sin \theta_i \sum_j A_{ij} \sin (\phi_i - \phi_j) h_0^2$$

$$C = \sum_{i,j} A_{ij} \sin (\phi_i - \phi_j) h_0^2$$

From (A-8) we can estimate the error in $\phi$ and $\theta$ as;

$$\Delta\phi = \text{Arctan} \frac{B}{A}$$

$$\Delta\theta = \text{Arcsin} \frac{A}{B} - \theta_0$$

(A-9)

Example of numerical calculation of $\Delta\phi$ and $\Delta\theta$ are shown in Fig. A-2 for $\phi_0 = 45°$, frequency $= 4$ kHz. Even when $\theta_0 = 80°$, $\theta_1$ is $62°$ and $\theta_2, \theta_3, \cdots$ take smaller values and the reflection coefficients of VLF waves at the ionosphere for those small angle of incidence is around 0.5. From the curves for $R = 0.5$ in Fig. A-2 we may conclude that for most case of direction measurements the errors in $\theta$ and $\phi$ are less than 10°.

## APPENDIX B

Design of antenna equalizing network

Usually, $E_z$ component is received by a vertical antenna which is equivalent to a series circuit of capacitance $C_a$ and voltage source $l \cdot E$ where $l$ is the height of antenna and $E$ is the intensity of wave electric field. The horizontal component of wave magnetic field is detected by two orthogonal loop antennas. The loop antenna is equivalent to the series circuit of the inductance $L_a$, resistance $r_{aa}$ and voltage source $V_l$. $V_l$ can be estimated in terms of wave electric field $E$ as;

$$V_l = -j\omega \frac{S_a N_a}{v_0} E$$

where $S_a$ is the area of $N_a$-turn loop antenna and $v_0$ is the light velocity. Generally these two type of antennas respond differently to the incident wave fields, so that additional CR network is required to equalize the response of the two antenna systems. In addition, the interference from radio broadcast has to be avoided by lowering the sensitivity at high frequency.

The parameters of antennas used in the present experiment are;

| | | |
|---|---|---|
| loop antenna | inductance | $L_a = 0.58$ mH |
| | resistance | $r_{aa} = 0.7$ ohm |
| | area | $S_a = 900 \ m^2$ |
| | turn | $N_a = 2$ |
| vertical antenna | height | $l = 6.375$ m |
| | capacitance | $C_a = 70.93$ pF |
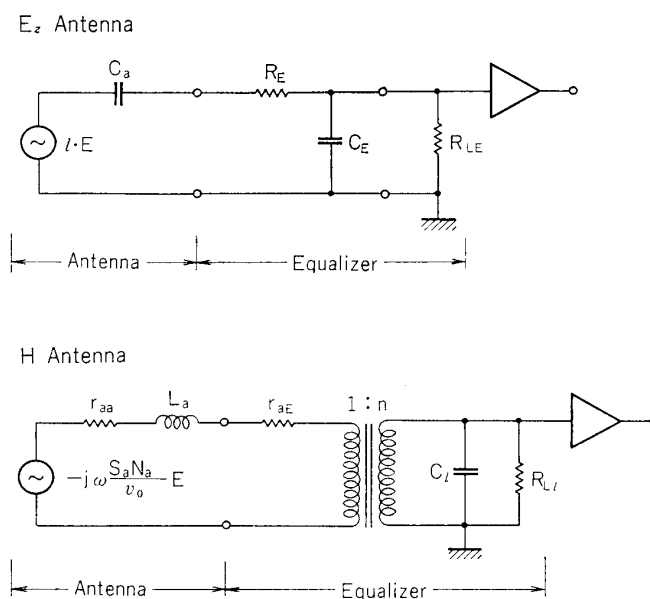
FIG. B-1.  Equalizing networks for $E_z$ and $H$ antennas.

The equalizing networks used in the present experiment are shown in Fig. B–1. The response of vertical antenna equalizer $Y_E(\omega)$ is given by;

$$Y_E(\omega) = \frac{j\omega C_a R_{LE}}{1 + j\omega\{(C_a + C_E)R_{LE} + C_a R_E\} - \omega^2 C_a C_E R_{LE} R_E} \tag{B-1}$$

and that of loop antenna $Y_l(\omega)$ is;

$$Y_l(\omega) = \frac{-j\omega n \dfrac{R'_{Ll}}{r_a + R'_{Ll}} \cdot \dfrac{S_a N_a}{v_0 l}}{1 + j\omega \dfrac{C'_l R'_{Ll} r_a + L_a}{r_a + R'_{Ll}} - \omega^2 \dfrac{C'_l R'_{Ll} L_a}{r_a + R'_{Ll}}} \tag{B-2}$$

where

$$r_a = r_{aa} + r_{aE}$$

$$R'_{Ll} = \frac{R_{Ll}}{n^2}$$

$$C'_l = n^2 C_l$$

Since $Y_E(\omega)$ must be equal to $Y_l(\omega)$ we obtain the following three equations;

$$C_a R_{LE} = \frac{n R'_{Ll} S_a N_a}{v_0(r_a + R'_{Ll}) \cdot l} = \frac{1}{\omega_0} \tag{B-3}$$

$$(C_a + C_E)R_{LE} + C_a R_E = \frac{C'_l R'_{Ll} r_a + L_a}{r_a + R'_{Ll}} = \frac{1}{\omega_1} \tag{B-4}$$
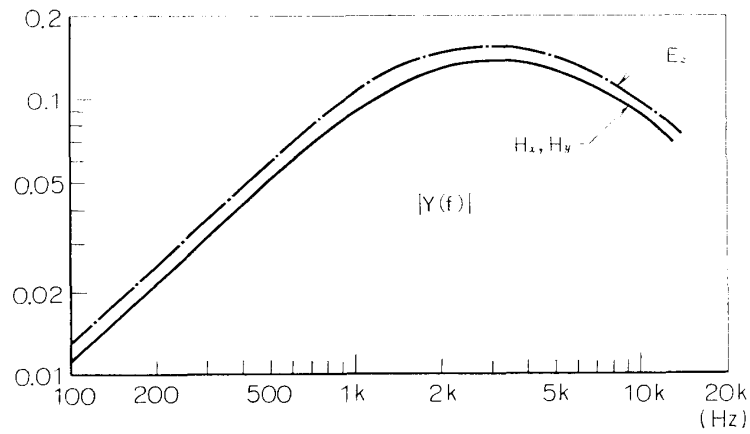
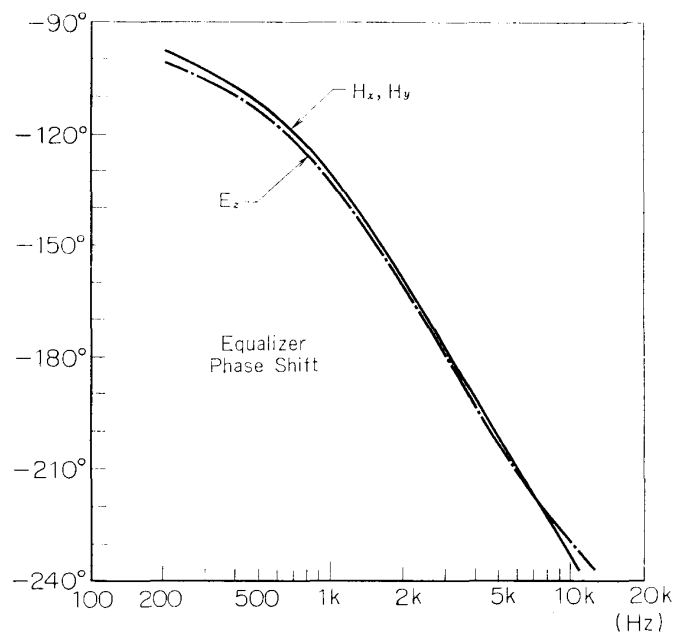Fig. B-2. Amplitude response of equalizing network and dummy antenna.



FIG. B-3. Phase shift due to the equalizing network and dummy antenna.

$$C_a R_{LE} C_E R_E = \frac{C_l' L_a R_{Ll}'}{r_a + R_{Ll}'} = \frac{1}{\omega_2^2} \qquad (\text{B-5})$$

Using three angular frequency $\omega_0, \omega_1$ and $\omega_2$, the response function can be written as;

$$Y(\omega) = \frac{\dfrac{\omega}{\omega_0}}{1 + j\dfrac{\omega}{\omega_1} - \dfrac{\omega^2}{\omega_2^2}} \qquad (\text{B-6})$$

$Y(\omega)$ shows $-6$ db/oct. band pass characteristics and the maximum of $|Y(\omega)|$ occurs at $\omega = \omega_2$. The maximum value of $|Y(\omega)|$ is $\omega_0/\omega_2$ and the $-3$ db frequencies $\omega_L$ and $\omega_H$ are expressed as;

$$\omega_L = \frac{\omega_2}{2}\left(\sqrt{\frac{\omega_2^2}{\omega_1^2}+4}-\frac{\omega_2}{\omega_1}\right)$$

$$\omega_H = \frac{\omega_2}{2}\left(\sqrt{\frac{\omega_2^2}{\omega_1^2}+4}+\frac{\omega_2}{\omega_1}\right)$$

Since (B–3), (B–4) and (B–5) are not independent ,the following inequality must be satisfied for all parameters of vertical antenna can be determined as real number.

$$\frac{1}{\omega_1}-\frac{1}{\omega_0} \geqq \frac{2}{\omega_2} \qquad (B-7)$$

(B–7) limits the allowable range of loop antenna parameters. We have chosen the parameters as;
      for loop antenna equalizer

$$r_{aE}=24.7 \text{ ohm}$$
$$n=100$$
$$C'_t=2000 \text{ pF}$$

      for vertical antenna equalizer

$$R_{LE}=259 \text{ kohm}$$
$$R_E=552 \text{ kohm}$$
$$C_E=273 \text{ pF}.$$

From above choice of parameters $f_0(=\omega_0/2\pi)=8.652$ KHz, $f_1=1.379$ KHz and $f_2=3.34$ KHz result. The lower cutoff frequency $f_L$ becomes 1.2 KHz and the upper cutoff frequency $f_H$ becomes 9.3 KHz. The maximum value of $|Y|$ becomes 0.159 at $f=3.34$ KHz. The response of equalizing network was measured by feeding the signal through dummy antennas. The results are shown in Fig. B–2 and B–3. As is seen from these figuresm a good agreement was attained over the frequency range of 0.5 to 9 kHz.

## REFERENCES

Bullough, K. and Sagredo, J. L., VLF goniometer observations at Halley Bay, Antarctica-I. The equipment and the measurement of signal bearing, Planet Space Sci., 21, 899, (1973).

Carpenter, D. L. and Stone, K., Direct detection by a whistler method of the magnetospheric electric field associated with a polar substorm, Planet. Space Sci., 15, 395, (1967).

Delloue, J., Garnier, M., Glangeaud, F. and Bildstein, P., La polarisation des sifflements radio-électriques en relation avec leur direction d'arrivée, C. r. held. Séanc. Acad. Sci., Paris, 257, 1131, (1963).

Ellis, G. R. A. and Cartwright, C. A., Directional observations of noise from the outer atmosphere, Nature, 184, 1307, (1959).

Maeda, K. and Kimura, I., A theoretical investigation of the propagation path of the whistling atmospherics, Rept. Ionos. Space Res., Japan, 10, 105, (1956).

Tanaka, Y., VLF hiss observed at Syowa station, Antarctica-I, Observation of VLF hiss, Proc. Res. Inst. Atmosph. Nagoya Univ., **19**, 33, (1972).

Watts, J. M., Direction finding on whistlers, J. Geophys. Res., **64**, 2029, (1959).

Yoshino, T., private communication.